

Synthesis and Properties of Polymers from Monosubstituted Acetylene Derivatives Bearing Ferroelectric Liquid Crystalline Groups

Hiromasa Goto,^{†,‡} Xiaoman Dai,[‡] Takenori Ueoka,[‡] and Kazuo Akagi^{*,†,‡,§}

Tsukuba Research Center for Interdisciplinary Materials Science (TIMS), Institute of Materials Science, Center for Tsukuba Advanced Research Alliance (TARA), University of Tsukuba, Tsukuba, Ibaraki 305-8573, Japan

Received November 25, 2003; Revised Manuscript Received February 10, 2004

ABSTRACT: Novel liquid crystalline polyacetylene derivatives were developed as advanced LC conjugated polymers with quick response to an electric field used as external force. In practice, we synthesized ferroelectric LC conjugated polymers by introducing fluorine-containing chiral LC groups into side chains of polyacetylenes. Phase-transition behaviors of these polymers were examined by differential scanning calorimetry and polarizing optical microscopy. Mesophases as well as higher order structures were evaluated with X-ray diffraction measurements. The polymers synthesized showed chiral nematic (N*), twist grain boundary smectic A (TGBA*), and chiral smectic (SmC*) phases in the heating and cooling processes. Observation of the SmC* phase allows us to expect that the polymer should exhibit ferroelectricity.

Introduction

Conjugated polymers with liquid crystalline (LC) groups in their side chains are currently drawing interest from the viewpoint of multifunctional electrical and optical materials.^{1–16} Polyacetylene is the simplest among all of the conjugate organic polymers, and after doping by iodine or AsF₅, it shows as high an electrical conductivity as metal. However, it is difficult to be characterized with standard experimental techniques due to its insolubility and infusibility. Various substituents have been introduced into the main chain, resulting in soluble and fusible polyacetylene derivatives. With introduction of LC groups into polyacetylene, it is expected that the orientation of the LC side chains may enhance the alignment of the main chain via the spontaneous orientation of the LC groups. The spontaneous orientation and externally forced alignment of the LC side chains enable us to control electrical and optical properties as well as their anisotropies.^{17–23} When an electric field is employed as an external force, ferroelectric LC (FLC) are more desirable than ordinary LC ones because the former are expected to respond more quickly to the electric field owing to their spontaneous polarization than the latter. The ferroelectric liquid crystallinity is due to spontaneous polarization generated in the chiral smectic C phase (SmC*) when it is surface stabilized. Recently, we synthesized polyacetylene derivatives substituted with chiroptical LC groups and confirmed the formation of the SmC* phase,^{21,23} although the liquid crystalline phase was unstable. Here, we synthesized advanced FLC polyacetylene derivatives with more thermally stable SmC* phase (Scheme 1). Polymer structures we synthesized in this report are summarized in Table 1

* To whom correspondence should be addressed.

[†] Tsukuba Research Center for Interdisciplinary Materials Science.

[‡] Institute of Materials Science.

[§] Center for Tsukuba Advanced Research Alliance.

Table 1. Polymer Structures

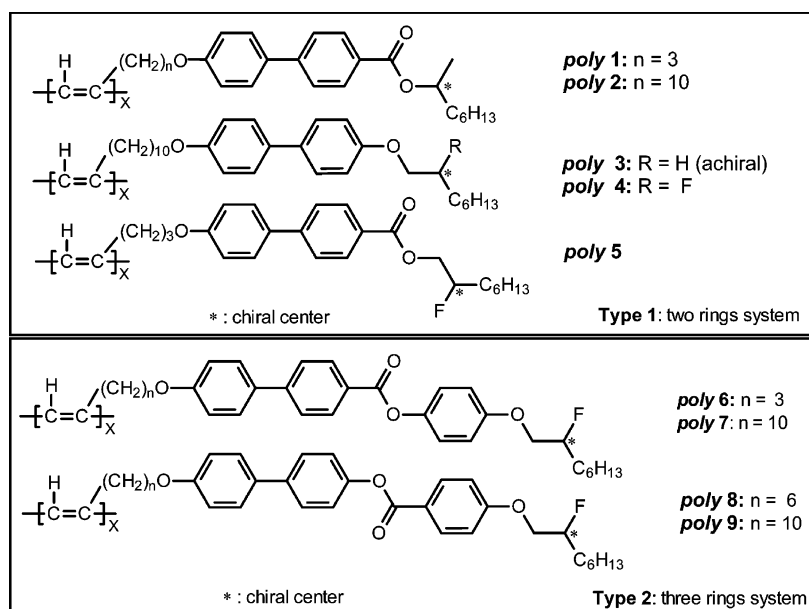
mesogen type	polymer	ring ^a	ester ^b	fluorine atom ^c	spacer length ^d
type 1	<i>poly-1</i>	2	1		3
	<i>poly-2</i>	2	1		10
	<i>poly-3</i>	2			10
	<i>poly-4</i>	2		1	10
	<i>poly-5</i>	2	1	1	3
type 2	<i>poly-6</i>	3	1	1	3
	<i>poly-7</i>	3	1	1	10
	<i>poly-8</i>	3	1	1	6
	<i>poly-9</i>	3	1	1	10

^a Number of phenylene rings in mesogenic core. ^b Number of ester groups in mesogen. ^c Number of fluorine atoms on chiral carbon. ^d Number of carbon atoms in alkyl chain.

Experimental Section

Techniques. All ¹H NMR and ¹³C NMR spectra were measured with a BRUKER AM500 FT-NMR spectrometer. CDCl₃ was used as a deuterated solvent, and TMS was used as an internal standard. ¹⁹F NMR spectra were recorded on a BRUKER AVANCE 500 spectrometer. To determine the chemical shifts of the ¹⁹F resonance, CF₃C₆H₅ was used as a standard ($\delta = -63.72$ ppm, referenced against CFCl₃ at 0.00 ppm). The 2D NMR analysis (¹H–¹³C and ¹H–¹⁹F NMR obtained by HMQC, heteronuclear multiquantum correlation spectroscopy, and HOESY, heteronuclear Overhauser effect spectroscopy, respectively) was carried out on selected samples for further confirmation of their structure. Infrared spectroscopic measurement was carried out with a Jasco FT-IR 550 spectrometer using KBr method. Phase-transition temperatures were determined using a Perkin-Elmer differential scanning calorimeter (DSC 7) apparatus at a constant heating/cooling rate of 10 °C/min, where first cooling and then heating processes were recorded. Optical texture observation was performed using a Nikon polarizing optical microscope equipped with a Linkam THMS 600 heating and cooling stage. Purities of intermediates and final compounds were checked by HPLC analysis. Molecular weights of the polymers were determined by gel permeation chromatography (GPC) with a Shodex A-80M column and a Jasco HPLC 870-UV detector with tetrahydrofuran (THF) used as the solvent. XRD measurements were performed with a Rigaku D-3F diffractometer in which X-ray power and scanning rate were set at 1200 mW and 5 deg/min, respec-

Scheme 1



tively. Molecular mechanics (MM) calculations for the polymers were carried out by a Silicon Graphics Cerius² system.

Materials. *N,N*-Dimethylformamide (DMF), tetrahydrofuran (THF), and CHCl_3 were distilled prior to use. The chiral alcohol (*S*)-(-)-2-fluorooctanol (**1**) was prepared according to the method reported by Nohira et al.²⁴ in which (*R*)-(+)-1,2-epoxyoctane was reacted with pyridinium poly(hydrogen fluoride) (DEAD), triphenylphosphine (TPP), 1,3-dicyclohexylcarbodiimide (DCC), and 4-dimethylaminopyridine (DMAP) were used as received from Tokyo Kasei (TCI).

Synthesis. 5-(4-Cyano-4'-biphenoxy)-1-pentyne (1). A mixture of 4-cyano-4'-hydroxybiphenyl (21.3 g, 0.11 mol), 5-chloro-1-pentyne (11.7 g, 0.11 mol), K_2CO_3 (15.2 g, 0.11 mol), and KI (1.82 g, 11 mmol) in 100 mL of DMF was refluxed for 72 h under an argon atmosphere. Then the solution was poured into a large amount of acetone, the solution was filtered off, and the filtrate was evaporated. The crude product was washed thoroughly with water and extracted with ether. The ether layer was dried over CaCl_2 overnight. After the organic solution was evaporated, the yellow solid was further purified by recrystallization from ethanol to afford 11.2 g of white powder (yield = 39%). IR (KBr, cm^{-1}): 3258 (s, $\nu_{\text{HC}\equiv}$), 2220 (s, ν_{CN}), 2100 (w, $\nu_{\text{C}=\text{C}}$), 1248 (s, ν_{COC}), 691 (m, $\gamma_{\text{HC}\equiv}$). ¹H NMR (500 MHz, CDCl_3 , δ from TMS, ppm): 1.97 (t, $J = 2.6$ Hz, 1H, $\text{HC}\equiv$), 2.03 (quint, $J = 6.4$ Hz, 2H, $\text{CH}_2\text{CH}_2\equiv\text{CH}$), 2.42 (dt, $J = 2.7$ Hz, 2H, $\text{HC}\equiv\text{CCH}_2$), 4.12 (t, $J = 6.2$ Hz, 2H, OCH_2), 7.01 (d, $J = 8.1$ Hz, 2H, ph), 7.51 (d, $J = 8.1$ Hz, 2H, ph), 7.61 (d, $J = 8.4$ Hz, 2H, ph), 7.68 (d, $J = 8.3$ Hz, 2H, ph). ¹³C NMR (125 MHz, CDCl_3 , δ from TMS, ppm): 15.13, 28.10, 66.29, 68.97, 83.01, 110.15, 115.12, 119.07, 127.11, 128.36, 131.57, 132.57, 145.24, 159.55. Anal. Calcd for $\text{C}_{18}\text{H}_{15}\text{NO}$: C, 82.73; H, 5.79; N, 5.36. Found: C, 82.66; H, 5.75; N, 5.33.

5-(4'-Biphenoxy-4-carboxylic acid)-1-pentyne (2). Compound **1** (8 g, 0.03 mol) was dissolved in a mixed solution of ethanol (150 mL) and water (100 mL). Then KOH (42 g, 0.75 mol) was added to the stirred mixture. The solution was refluxed for 72 h at 60 °C. After the organic solvent was evaporated, the residue solution was neutralized with 1 N HCl and stirred overnight. The solution was filtered to give 5.2 g of white solid (yield = 62%). IR (KBr, cm^{-1}): 3305 (s, $\nu_{\text{HC}\equiv}$), 2860, 2672, 2551 (m, br, ν_{COOH}), 1683 (s, $\nu_{\text{C}=\text{O}}$), 1274 (s, ν_{COC}), 633 (m, $\gamma_{\text{HC}\equiv}$). ¹H NMR (500 MHz, CDCl_3 , δ from TMS, ppm): 1.97 (t, $J = 2.6$ Hz, 1H, $\text{HC}\equiv$), 2.03 (quint, $J = 6.4$ Hz, 2H, $\text{CH}_2\text{CH}_2\equiv\text{CH}$), 2.60 (dt, $J = 2.8$ Hz, 2H, $\text{HC}\equiv\text{CCH}_2$), 4.15 (t, $J = 6.2$ Hz, 2H, OCH_2), 7.28 (d, $J = 8.1$ Hz, 2H, ph), 7.63 (d, $J = 8.4$ Hz, 2H, ph), 7.72 (d, $J = 8.3$ Hz, 2H, ph), 7.95 (d, $J = 8.3$ Hz, 2H, ph). ¹³C NMR (125 MHz, CDCl_3 , δ from TMS,

ppm): 15.17, 29.00, 66.29, 69.00, 83.32, 115.13, 119.10, 127.21, 128.31, 131.85, 132.58, 145.32, 159.64, 167.7.

8-Bromo-1-octyne (3). A solution of sodium acetylide (44 g, 18 wt % in xylene, 0.16 mol) was very slowly added to a solution of 1,6-dibromohexane (120 g, 0.49 mol) in 60 mL of DMF by pressure-equalized dropping funnel. The reaction mixture was refluxed for 24 h at 50 °C. The precipitate was removed by filtration, and the solvent was evaporated. Vacuum distillation afforded 20.2 g of colorless oily product (70–73 °C/4 mmHg). Yield = 67%. IR (KBr, cm^{-1}): 3305 ($\nu_{\text{CH}\equiv}$), 2117 (w, $\nu_{\text{C}=\text{C}}$), 636 (m, $\gamma_{\text{HC}\equiv}$). ¹H NMR (500 MHz, CDCl_3 , δ from TMS, ppm): 1.26–1.62 (m, 6H, CH_2), 1.86 (t, $J = 2.6$ Hz, 1H, $\text{HC}\equiv$), 2.14 (m, 2H, $\text{HC}\equiv\text{CCH}_2$), 2.81 (m, 2H, $\text{CH}_2\text{CH}_2\text{Br}$), 3.46 (t, $J = 6.9$ Hz, 2H, CH_2Br). ¹³C NMR (125 MHz, CDCl_3 , δ from TMS, ppm): 18.43, 27.44, 28.05, 28.43, 32.80, 33.98, 66.51, 84.72.

12-Bromo-1-dodecyne (4). This compound was prepared using a method similar to that described for **2**. Quantity used: sodium acetylide (40.0 g, 18 wt % in xylene, 0.15 mol), 1,10-dibromodecane (40.0 g, 0.13 mol), DMF (20 mL). Vacuum distillation afforded a colorless oily product (130–134 °C/4 mmHg; yield, 64.2%, 18.9 g). IR (KBr, cm^{-1}): 3300 (s, $\nu_{\text{CH}\equiv}$), 2110 (w, $\nu_{\text{C}=\text{C}}$), 643 (m, $\gamma_{\text{HC}\equiv}$). ¹H NMR (500 MHz, CDCl_3 , δ from TMS, ppm): 1.29–1.88 (m, 16H), 1.93 (t, $J = 2.6$ Hz, 1H, $\text{HC}\equiv$), 2.17 (m, 2H, $\text{HC}\equiv\text{CCH}_2$), 3.40 (t, $J = 6.9$ Hz, 2H, CH_2Br). ¹³C NMR (125 MHz, CDCl_3 , δ from TMS, ppm): 16.39, 28.14, 28.71, 29.05, 29.07, 29.31, 29.37, 29.42, 32.83, 33.96, 66.08, 84.73.

12-(4'-Biphenoxy-4-carboxylic acid)-1-dodecyne (5). A solution of 4'-hydroxybipheny-4-carboxylic acid (25 g, 0.12 mol), KI (2 g, 0.012 mol) and KOH (50 g, 0.9 mol) in water (100 mL) and ethanol (160 mL) was stirred for 15 h at room temperature. Then compound **4** (7.15 g, 0.03 mol) was added, and the solution was refluxed for 1 week at 55 °C. The solution was allowed to cool to room temperature, and ether was added to the solution. The organic layer was washed with water thoroughly and dried over CaCl_2 . After evaporation of the solvent, the crude product was recrystallized from acetone to afford 28 g of white powder (yield = 61%). IR (KBr, cm^{-1}): 3295 (s, $\nu_{\text{HC}\equiv}$), 2868, 2666, 2546 (m, ν_{COOH}), 2113 (w, $\nu_{\text{C}=\text{O}}$), 1681 ($\nu_{\text{C}=\text{O}}$), 1294 ($\nu_{\text{C}=\text{C}}$), 655 (m, $\gamma_{\text{HC}\equiv}$). ¹H NMR (500 MHz, CDCl_3 , δ from TMS, ppm): 1.22–1.77 (m, 16H), 1.94 (t, $J = 2.8$ Hz, 1H, $\text{HC}\equiv$), 2.17 (m, 2H, $\text{HC}\equiv\text{CCH}_2$), 3.98 (t, $J = 6.6$ Hz, 2H, CH_2Br), 6.67 (d, $J = 8.1$ Hz, 2H, ph), 6.69 (d, $J = 8.4$ Hz, 2H, ph), 7.41 (d, $J = 8.4$ Hz, 2H, ph), 7.45 (d, $J = 8.1$ Hz, 2H, ph). ¹³C NMR (125 MHz, CDCl_3 , δ from TMS, ppm): 16.31, 26.02, 28.50, 28.74, 29.06, 29.32, 29.37, 29.42, 29.50, 29.74, 66.10, 84.79, 114.75, 115.45, 127.66, 127.95, 133.21, 133.84, 144.57,

154.59, 167.71.

(S)-2-Fluorooctanol (6). To a stirred solution of pyridinium poly(hydrogen fluoride) (25 mL) in a Teflon flask was added dropwise via a syringe (*R*)-1,2-epoxyoctane (9.66 g, 75.5 mmol) in ether (37 mL) at 0 °C. The solution was stirred for 5 h under an argon atmosphere. Then the reaction mixture was poured into ~100 mL of crushed ice water. The crude product was extracted by ether and washed with water several times with a Teflon separating funnel. The organic layer was neutralized by saturated NaHCO₃ solution and dried over anhydrous sodium sulfate. The solvent was removed by evaporation. Final purification by vacuum distillation yielded 5.90 g (yield = 53.1%) of **6** as colorless liquid (68–72 °C at 6 mmHg). IR (cm⁻¹): 3398 (m, ν_{OH}), 2929, 2859 (s, ν_{CH₂}). ¹H NMR (500 MHz, CDCl₃, δ from TMS, ppm): 0.89 (t, 3H, *J* = 6.9 Hz, CH₃), 1.29–1.72 (m, 10H, CH₂C*HF(CH₂)₅CH₃), 2.56 (s, 1H, OH), 3.60–3.73 (m, 2H, C*HFCH₂OH), 4.49–4.63 (dm, 1H, *J*_{HF} = 49.81 Hz, OCH₂C*HF). ¹³C NMR (125 MHz, CDCl₃, δ from TMS, ppm): 14.05, 22.58, 24.97, 29.13, 30.93, 31.69, 64.97, 94.8 (d, *J*_{CF} = 167.7 Hz).

4-(8-Octyloxy)-4'-biphenol (7). Compound **3** (12.0 g, 63.5 mmol) in acetone (30 mL) was added dropwise to a stirred refluxing suspension consisting of 4,4'-biphenyldiol (35.4 g, 190 mmol) and anhydrous potassium carbonate (26.2 g, 190 mmol) in 2-butanone (400 mL). After the addition was completed, the solution was heated under reflux for 24 h. The precipitated potassium bromide and the excess of potassium carbonate were removed by filtration, and the filtrate was evaporated. Purification by column chromatography (silica gel, hexane/ethyl acetate = 2) and recrystallization from ethanol afforded 18 g (yield = 96%) of white solid. IR (KBr, cm⁻¹): 3290 (m, ν_{OH}), 2110 (w, ν_{C=C}), 1255 (s, ν_{COC}). ¹H NMR (500 MHz, CDCl₃, δ from TMS, ppm): 1.25–1.82 (m, 8H, CH₂), 1.95 (t, *J* = 2.7 Hz, 1H, HC≡), 2.19 (m, 2H, HC≡CCH₂), 3.96 (t, 2H, *J* = 6.5 Hz, OCH₂), 4.73 (s, 1H, OH), 6.78 (d, *J* = 8.7 Hz, ph), 6.92 (d, 2H, *J* = 8.7 Hz, ph), 7.50 (d, 2H, *J* = 8.6 Hz, ph), 7.34 (d, 2H, *J* = 8.7 Hz, ph). ¹³C NMR (125 MHz, CDCl₃, δ from TMS, ppm): 18.41, 26.05, 28.73, 29.31, 29.51, 68.05, 68.73, 84.80, 114.72, 115.31, 127.45, 127.74, 133.23, 133.65, 144.59, 154.58.

4-(12-Dodecyloxy)-4'-biphenol (8). Compound **4** (9.24 g, 38 mmol) in 2-butanone (30 mL) was added dropwise to a stirred refluxing suspension consisting of 4,4'-biphenyldiol (50.0 g, 269 mmol), anhydrous potassium carbonate (53.8 g, 389 mmol), and 2-butanone (500 mL). Once the addition was complete, the reaction solution was heated under reflux for 24 h. The precipitated potassium bromide and the excess of potassium carbonate were filtered off, and the filtrate was evaporated to give a solid. Purification by column chromatography (silica gel, hexane/ethyl acetate = 2) and recrystallization from ethanol afforded 7.17 g (53.9%) of white solid. Mp = 137–140 °C. IR (KBr, cm⁻¹): 3289 (m, ν_{OH}), 2112 (w, ν_{C=C}), 1252 (ν_{COC}). ¹H NMR (500 MHz, CDCl₃, δ from TMS, ppm): 1.25–1.82 (m, 16H, CH₂), 1.94 (t, *J* = 2.7 Hz, 1H, HC≡), 2.18 (m, 2H, HC≡CCH₂), 3.98 (t, 2H, *J* = 6.5 Hz, OCH₂), 4.76 (s, 1H, OH), 6.88 (d, 2H, *J* = 8.7 Hz, ph), 6.94 (d, 2H, *J* = 8.7 Hz, ph), 7.42 (d, 2H, *J* = 8.6 Hz, ph), 7.45 (d, 2H, *J* = 8.7 Hz, ph). ¹³C NMR (125 MHz, CDCl₃, δ from TMS, ppm): 18.41, 26.06, 28.49, 28.75, 29.09, 29.31, 29.37, 29.51, 29.12, 68.05, 68.71, 84.80, 114.78, 115.58, 127.66, 127.94, 133.22, 133.63, 144.57, 154.57.

1-Phenyl methoxy-4-((S)-2-fluoro-octyloxy)benzene (9). A solution of 4-benzyloxyphenol (4 g, 20 mmol) and DEAD (8.7 g, 20 mmol) in 20 mL of THF was added to a solution of TPP (5.3 g, 20 mmol) and **6** (2.2 g, 15 mmol) in THF (25 mL) by a pressure-equalized dropping funnel. After completion of the addition, the solution was stirred for 72 h. Then the solvent was evaporated, and the crude product was purified by column chromatography (silica gel, *n*-hexane/ethyl acetate = 2) and recrystallized from acetone to afford 3.8 g (yield = 78%) of white crystal. IR (KBr, cm⁻¹): 1260 (s, ν_{COC}). ¹H NMR (500 MHz, CDCl₃, δ from TMS, ppm): 0.89 (t, *J* = 7.0 Hz, 3H, CH₃), 1.29–1.72 (m, 10H, CH₂), 4.64 (br, ph-CH₂O-ph), 3.94–4.06 (m, 2H, OCH₂), 4.77 (*J*_{HF} = 49.1 Hz, OCH₂C*HF), 6.63 (d, *J* = 7.2 Hz, 2H, ph), 6.90 (d, *J* = 7.2 Hz, 2H, ph), 7.23 (t, *J* = 6.58, 1H, ph), 7.29 (d, *J* = 7.1 Hz, 2H, ph), 7.40 (d, *J* = 7.3 Hz, 2H,

ph). ¹³C NMR (125 MHz, CDCl₃, δ from TMS, ppm): 14.04, 22.56, 24.64, 29.01, 31.52, 31.67, 70.51, 70.71, 92.07 (d, *J*_{CF} = 171.5 Hz), 115.71, 115.71, 127.47, 127.60, 128.55, 137.27, 153.00, 153.37.

4-((S)-2-Fluoro-octyloxy)phenol (10). Compound **9** (3 g, 12 mmol) was treated with palladium carbon in methanol (50 mL) under hydrogen gas flow for 2 days. After completion of the reaction, the crude product was purified by column chromatography (silica gel, *n*-hexane/ethyl acetate = 2) to afford 1.8 g (yield = 61%) of white crystal. IR (KBr, cm⁻¹): 3290 (m, ν_{OH}), 1261 (ν_{COC}). ¹H NMR (500 MHz, CDCl₃, δ from TMS, ppm): 0.69 (t, *J* = 7.3 Hz, 3H, CH₃), 1.28–1.72 (m, 10H, CH₂), 3.96–4.03 (m, 2H, CH₂), 4.78 (dm, 1H, *J*_{HF} = 49.1 Hz, OCH₂C*HF), 6.02 (s, 1H, OH), 6.74 (d, 2H, 7.2 Hz, ph), 6.61 (d, 2H, 7.3 Hz, ph). ¹³C NMR (125 MHz, CDCl₃, δ from TMS, ppm): 13.99, 16.77, 22.56, 29.09, 31.51, 31.66, 70.66, 92.15 (d, *J*_{CF} = 171.4 Hz), 115.9, 116.2, 150.46, 152.55.

Ethyl 4-[(S)-2-Fluoro-octyloxy]benzoate (11). To a mixture of ethyl *p*-hydroxybenzoate (6.00 g, 36 mmol) and 9.44 g (36 mmol) of triphenylphosphine (TPP) in 80 mL of THF was added dropwise a solution of 16.0 g (in toluene solution, 36 mmol) of diethyl azodicarboxylate (DEAD), 4.44 g (30 mmol) of **6**, and 90 mL of THF. The reaction mixture was stirred at room temperature overnight. The precipitate was removed by filtration, the filtrate was evaporated to remove the solvent, and the residue was purified by column chromatography (silica gel, hexane/ethyl acetate = 2/1). The crude product was recrystallized from an ethyl acetate:hexane mixture and dried under vacuum to afford 8.01 g of **7** as white solid in 90.2% yield. Mp = 47–48 °C. IR (KBr, cm⁻¹): 1680 (ν_{C=O}). ¹H NMR (500 MHz, CDCl₃, δ from TMS, ppm): 0.89 (t, 3H, *J* = 6.8, CH₃), 1.23–1.78 (m, 10H, CH₂), 4.04–4.13 (m, 2H, OCH₂), 4.33 (q, 2H, *J* = 7.1 Hz, CH₂), 4.82 (dm, 1H, *J*_{HF} = 51.7 Hz, OCH₂C*HF), 6.93 (d, 2H, *J* = 6.9 Hz, ph), 7.99 (d, 2H, *J* = 8.9 Hz). ¹³C NMR (125 MHz, CDCl₃, δ from TMS, ppm): 14.00, 14.39, 22.56, 24.89, 29.10, 31.74, 60.57, 69.79, 91.71 (d, *J*_{CF} = 172.5 Hz), 114.18, 115.29, 131.60, 162.26, 166.24.

4-[(S)-2-Fluoro-octyloxy]benzoic acid (12). Compound **11** (4.00 g, 13.5 mmol) was hydrolyzed by heating it in a solution of NaOH (2.69 g, 67 mmol) in a mixed solution of 15 mL of water (15 mL) and methanol (24 mL) for 4 h at 50 °C. The methanol was evaporated, and the residue solution was diluted with water and acidified to pH = 2 with 2 N hydrochloric acid. The solution was extracted with ether, washed with water thoroughly, and dried over anhydrous sodium sulfate. The ether layer was removed by evaporation and dried under reduced pressure. Product **5** was obtained as white solid in 98.1% yield (3.55 g). IR (KBr, cm⁻¹): 2863, 2673, 2564 (br, s, ν_{COOH}), 1685 (ν_{C=O}). ¹H NMR (500 MHz, CDCl₃, δ from TMS, ppm): 0.90 (t, *J* = 6.9 Hz, 3H, CH₃), 1.25–1.86 (m, 10H, CH₂), 4.08–4.17 (m, 2H, OCH₂), 4.84 (dm, 1H, *J*_{HF} = 51.7 Hz, OCH₂C*HF), 6.97 (d, 2H, *J* = 8.9 Hz, ph), 8.07 (d, 2H, *J* = 8.9 Hz, ph). ¹³C NMR (125 MHz, CDCl₃, δ from TMS, ppm): 14.04, 22.55, 24.84, 29.17, 31.43, 31.65, 69.99, 91.64 (d, *J*_{CF} = 172.5 Hz), 114.21, 115.36, 132.45, 162.98, 171.40.

(R)-(-)-1-Methylheptyl-4'-pentynoxybiphenyl-4-carboxylate (mono-1). Into a 100 mL three-necked round-bottom flask was placed **2** (2.5 g, 8.9 mmol) and DEAD (3.87 g, 8.9 mmol) in 30 mL of THF under argon. Then (*S*)-octanol (1.45 mL) and TPP (2.33 g, 8.9 mmol) in 20 mL of THF was added to the solution by a pressure-equalized dropping funnel. After the reaction mixture was stirred for 12 h, the solution was extracted by CHCl₃ and washed with water thoroughly. The solution was dried by CaCl₂ overnight. Recrystallization from ethanol afforded 2.8 g of white crystals of **mono-1** (yield = 81%). [α]_D²⁶: -34.5°. IR (KBr, cm⁻¹): 3310 (s, ν_{HC≡}), 2120 (w, ν_{C=C}), 1700 (s, ν_{C=O}), 640 (m, γ_{HC≡}). ¹H NMR (500 MHz, CDCl₃, δ from TMS, ppm): 0.87 (t, 3H, *J* = 7 Hz, CH₃), 1.28–1.80 (m, 13H, CH₂, CH₃), 1.98 (t, 1H, *J* = 2.5 Hz, HC≡), 2.01 (m, 2H, HC≡CCH₂), 2.43 (m, 2H, CH₂), 4.12 (t, 2H, *J* = 6.09 Hz, OCH₂), 5.16 (sextet, 1H, *J* = 6.1 Hz, COOC*HCH₃), 6.99 (d, 2H, *J* = 8.7 Hz, ph), 7.55 (d, 2H, *J* = 7.3 Hz, ph), 7.61 (d, 2H, *J* = 7.2 Hz, ph), 8.07 (d, 2H, *J* = 9.4 Hz, ph). ¹³C NMR (125 MHz, CDCl₃, δ from TMS, ppm): 14.01, 15.19, 20.12, 22.60, 25.44, 28.18, 29.19, 31.77, 36.13, 66.28, 68.98, 71.67, 83.37,

114.98, 126.42, 128.36, 129.09, 130.05, 132.62, 145.03, 159.15, 166.17. ^{19}F NMR (470 MHz, CDCl_3 , δ , ppm): -186.45.

(R)-(-)-1-Methylheptyl-4'-decyloxybiphenyl-4-carboxylate (mono-2). This compound was prepared using a method similar to that described for **mono-1**. Quantity used: **5** (1 g, 2.64 mmol) and DEAD (1.15 g, in toluene, 2.64 mmol) in THF (3 mL); (*S*)-octanol (0.43 mL) and TPP (0.7 g, 2.64 mmol) in THF (2 mL). Yield: 75%, 0.97 g (pale orange solid). IR (KBr, cm^{-1}): 3320 (s, $\nu_{\text{HC}\equiv}$), 2130 (w, $\nu_{\text{C}=\text{C}}$), 1700 (s, $\nu_{\text{C}=\text{O}}$), 640 (m, $\gamma_{\text{HC}\equiv}$). ^1H NMR (500 MHz, CDCl_3 , δ from TMS, ppm): 0.87 (t, 3H, $J = 6.7$ Hz, CH_3), 1.18–1.81 (m, 29H, CH_2 , CH_3), 1.93 (t, 1H, $J = 2.5$ Hz, $\text{HC}\equiv$), 2.17 (m, 2H, $\text{HC}\equiv\text{CCH}_2$), 3.98 (t, 2H, $J = 6.52$, OCH_2), 5.16 (sextet, 1H, $J = 6.6$ Hz, $\text{COOC}^*\text{HCH}_3$), 6.98 (d, 2H, $J = 7.4$ Hz, ph), 7.04 (d, 2H, $J = 6.8$ Hz, ph), 7.01 (d, 2H, $J = 7.0$ Hz, ph), 8.06 (d, 2H, $J = 8.3$ Hz, ph). ^{13}C NMR (125 MHz, CDCl_3 , δ from TMS, ppm): 13.99, 15.16, 18.33, 20.04, 22.53, 25.55, 25.97, 26.15, 28.67, 29.11, 29.25, 29.35, 29.46, 31.69, 32.75, 36.05, 65.98, 70.71, 71.57, 84.67, 114.86, 126.30, 128.23, 128.93, 129.95, 132.22, 145.03, 159.34, 166.11.

4-Octoxy-4'-(12-dodecyloxy)biphenyl (mono-3). This compound was prepared using a method similar to that described for **mono-1**. Quantity used: DEAD (5.66 g, in toluene 13.0 mmol) and 1-octanol (1.26 g, 9.7 mmol) in THF (30 mL); **8** (3.00 g, 8.5 mmol) and TPP (3.34 g, 13.7 mmol) in THF (15 mL). Yield: 46%, 1.82 g (white solid). Mp = 114–117 °C. IR (KBr, cm^{-1}): 3287 (m, $\nu_{\text{HC}\equiv}$), 2110 (w, $\nu_{\text{C}=\text{C}}$), 1251 (s, ν_{COC}), 637 (w, $\gamma_{\text{HC}\equiv}$). ^1H NMR (500 MHz, CDCl_3 , δ from TMS, ppm): 0.90 (t, 3H, $J = 6.9$ Hz, CH_3), 1.25–1.89 (m, 28H, CH_2), 1.94 (t, 1H, $J = 2.7$ Hz, $\text{HC}\equiv$), 2.19 (m, 2H, $\text{HC}\equiv\text{CCH}_2$), 3.99 (t, 4H, $J = 6.6$ Hz, OCH_2), 6.94 (d, 4H, $J = 8.7$ Hz, ph), 7.46 (d, 4H, $J = 8.7$ Hz, ph). ^{13}C NMR (125 MHz, CDCl_3 , δ from TMS, ppm): 14.10, 14.69, 16.41, 22.67, 26.06, 26.08, 28.17, 28.75, 29.09, 29.38, 29.43, 29.45, 29.51, 31.63, 32.64, 33.99, 66.05, 66.12, 84.79, 114.77, 127.65, 133.35, 158.26.

4-[(S)-2-Fluorooctoxy]-4'-(12-dodecyloxy)biphenyl (mono-4). This compound was prepared using a method similar to that described for **mono-1**. Quantity used: **8** (2 g, 5.7 mmol) and DEAD (3.70 g, in toluene, 8.5 mmol) in THF (10 mL); TPP (2.33 g, 8.5 mmol) and **6** (0.84 g, 5.7 mmol) in THF (20 mL). Yield: 59.5%, 1.62 g (white solid). Mp = 112–113 °C. IR (KBr, cm^{-1}): 3286 (m, $\nu_{\text{HC}\equiv}$), 2112 (w, $\nu_{\text{C}=\text{C}}$), 1251 (s, ν_{COC}), 634 (w, $\gamma_{\text{HC}\equiv}$). ^1H NMR (500 MHz, CDCl_3 , δ from TMS, ppm): 0.90 (t, 3H, $J = 6.9$, CH_3), 1.24–1.94 (m, 26H), 1.94 (t, 1H, $J = 2.7$ Hz, $\text{HC}\equiv$), 2.19 (m, 2H, $\text{HC}\equiv\text{CCH}_2$), 3.98 (t, 2H, $J = 6.6$ Hz, OCH_2), 4.10 (m, 2H, $\text{OCH}_2\text{C}^*\text{HF}$), 4.83 (dm, 1H, $J_{\text{HF}} = 49.6$ Hz, $\text{OCH}_2\text{C}^*\text{HF}$), 6.94 (d, 2H, $J = 8.7$ Hz, ph), 6.96 (d, 2H, $J = 8.7$ Hz, ph), 7.46 (d, 2H, $J = 8.6$ Hz, ph), 7.47 (d, 2H, $J = 8.7$ Hz, ph). ^{13}C NMR (125 MHz, CDCl_3 , δ from TMS, ppm): 14.05, 18.41, 22.56, 24.54, 24.88, 26.07, 28.50, 28.76, 29.09, 29.32, 29.51, 31.64, 31.67, 31.70, 46.51, 66.11, 69.58, 70.05, 84.60, 92.00 (d, $J_{\text{CF}} = 171.6$ Hz), 114.78, 127.72, 133.17, 134.10, 144.57, 148.48, 157.67, 158.32. ^{19}F NMR (470 MHz, CDCl_3 , δ , ppm): -187.74.

(S)-2-Fluorooctyl-4'-pentynoxybiphenyl-4-carboxylate (mono-5). This compound was prepared using a method similar to that described for **mono-1**. Quantity used: **2** (1.4 g, 5 mmol) and DEAD (2.17 g, in toluene, 5 mmol) in THF (3 mL); **6** (0.74 g, 5 mmol) and TPP (1.3 g, 5 mmol) in THF (3 mL). Yield: 51%, 1.08 g (white solid). IR (KBr, cm^{-1}): 3300 (m, $\nu_{\text{HC}\equiv}$), 2130 (w, $\nu_{\text{C}=\text{C}}$), 1730 (s, $\nu_{\text{C}=\text{O}}$), 1250 (s, ν_{COC}), 640 (w, $\gamma_{\text{HC}\equiv}$). ^1H NMR (500 MHz, CDCl_3 , δ from TMS, ppm): 0.90 (t, 3H, 7.0 Hz, CH_3), 1.35–1.58 (m, 10 H, CH_2), 1.86 (t, 1H, $J = 2.6$ Hz, $\text{HC}\equiv$), 2.03 (m, 2H, $\text{HC}\equiv\text{CCH}_2$), 2.44 (m, 2H, CH_2), 4.13 (t, 2H, $J = 6.1$ Hz, OCH_2), 4.44 (m, 2H, $\text{OCH}_2\text{C}^*\text{HF}$), 4.82 (dm, 1H, $J = 48.7$ Hz, $\text{OCH}_2\text{C}^*\text{HF}$), 7.01 (d, 2H, $J = 7.1$ Hz, ph), 7.5 Hz (d, 2H, $J = 6.9$ Hz, ph), 7.63 (d, 2H, $J = 7.2$ Hz, ph), 8.12 (d, 2H, $J = 8.4$ Hz, ph). ^{13}C NMR (125 MHz, CDCl_3 , from TMS, ppm): 14.04, 15.19, 22.55, 24.79, 28.17, 29.05, 31.43, 31.63, 66.16, 66.28, 68.96, 83.37, 91.53 (d, $J_{\text{CF}} = 172.0$ Hz), 115.00, 126.52, 127.69, 128.40, 130.29, 132.43, 145.52, 159.24, 166.30. ^{19}F NMR (470 MHz, CDCl_3 , δ , ppm): -187.74.

4-((S)-2-Fluorooctyloxy)-phenyl-4'-pentyl-4-biphenyl-carboxylate (mono-6). A solution of **2** (1.4 g, 5 mmol), **10** (0.8 g, 5 mmol), DCC (1.1 g, 5 mmol), and DMAP (0.64 g, 5 mmol) in 80 mL of CH_2Cl_2 and 30 mL of THF was stirred for

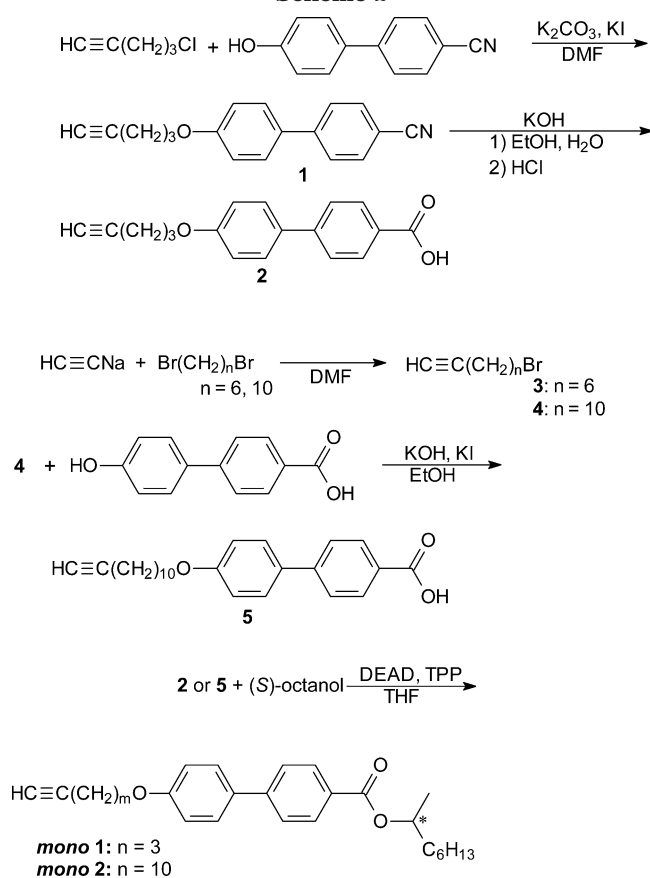
1 week at room temperature. Then the insoluble fraction of the solution was filtered off, and the filtrate was purified by column chromatography (silica gel, benzene) to afford 1.5 g of white crystal (yield = 61%). $[\alpha]_{\text{D}}^{27}$: +3.0°. IR (KBr, cm^{-1}): 3300 (m, $\nu_{\text{HC}\equiv}$), 2130 (w, $\nu_{\text{C}=\text{C}}$), 1730 (s, $\nu_{\text{C}=\text{O}}$), 1252 (s, ν_{COC}), 640 (w, $\gamma_{\text{HC}\equiv}$). ^1H NMR (500 MHz, CDCl_3 , δ from TMS, ppm): 0.90 (t, 3H, $J = 7.1$ Hz, CH_3), 1.30–1.71 (m, 10H, CH_2), 1.82 (t, 1H, $J = 2.6$ Hz, $\text{HC}\equiv$), 1.85 (m, 2H, CH_2), 2.23 (m, 2H, $\text{HC}\equiv\text{CCH}_2$), 4.13 (m, 4H, OCH_2 , $\text{OCH}_2\text{C}^*\text{HF}$), 4.80 (dm, 1H, $J_{\text{HF}} = 49.5$ Hz, $\text{CH}_2\text{C}^*\text{HF}$), 6.95 (d, $J = 2\text{H}$, 6.9 Hz, ph), 7.02 (d, 2H, $J = 7.5$ Hz, ph), 7.58 (d, 2H, $J = 7.3$ Hz, ph), 7.67 (d, 2H, $J = 7.4$ Hz, ph), 8.22 (d, 2H, 8.5 Hz, $J = 8.5$ Hz, ph). ^{13}C NMR (125 MHz, CDCl_3 , δ from TMS, ppm): 14.06, 15.19, 22.57, 24.88, 28.17, 29.02, 31.50, 31.60, 67.98, 70.22, 70.41, 83.37, 91.93 (d, $J_{\text{CF}} = 171.9$ Hz), 115.04, 115.39, 122.59, 126.62, 127.65, 128.44, 130.70, 132.32, 144.91, 145.88, 156.33, 159.34, 171.49. ^{19}F NMR (470 MHz, CDCl_3 , δ , ppm): -187.55.

4-((S)-2-Fluorooctyloxy)-phenyl-4'-dodecyloxy-4-biphenyl-carboxylate (mono-7). This compound was prepared using a method similar to that described for **mono-6**. Quantity used: **5** (0.52 g, 1.3 mmol), **10** (1.3 g, 1.4 mmol), DCC (0.46 g, 2.2 mmol), and DMAP (0.27 g, 2.2 mmol) in CH_2Cl_2 (40 mL). Yield: 63%, 0.5 g (white crystal). IR (KBr, cm^{-1}): 3300 (m, $\nu_{\text{HC}\equiv}$), 2130 (w, $\nu_{\text{C}=\text{C}}$), 1730 (s, $\nu_{\text{C}=\text{O}}$), 1252 (s, ν_{COC}), 640 (w, $\gamma_{\text{HC}\equiv}$). ^1H NMR (500 MHz, CDCl_3 , δ from TMS, ppm): 0.90 (t, 3H, $J = 7.0$ Hz, CH_3), 1.25–1.70 (m, 26H, CH_2), 1.93 (t, 1H, $J = 2.6$ Hz, $\text{HC}\equiv$), 2.16 (m, 2H, $\text{HC}\equiv\text{CCH}_2$), 4.02 (m, 4H, OCH_2 , $\text{OCH}_2\text{C}^*\text{HF}$), 4.83 (dm, 1H, $J_{\text{HF}} = 49.8$ Hz, $\text{OCH}_2\text{C}^*\text{HF}$), 6.98 (m, 4H, ph), 7.13 (d, 2H, $J = 7.1$ Hz, ph), 7.58 (d, 2H, $J = 7.5$ Hz, ph), 7.88 (d, 2H, $J = 8.3$ Hz, ph), 8.22 (d, 2H, $J = 8.4$ Hz, ph). ^{13}C NMR (125 MHz, CDCl_3 , δ from TMS, ppm): 14.05, 18.42, 18.78, 21.91, 21.57, 24.65, 25.63, 28.78, 29.10, 29.27, 29.38, 29.44, 29.52, 31.51, 31.65, 68.16, 70.23, 70.42, 83.34, 91.93 (d, $J_{\text{CF}} = 171.5$ Hz), 115.03, 115.39, 122.80, 126.59, 127.59, 128.40, 130.69, 132.04, 144.92, 145.97, 156.33, 159.62, 171.50. ^{19}F NMR (470 MHz, CDCl_3 , δ , ppm): -187.54.

4-[4-((S)-2-Fluorooctyloxy)benzyloxy]-4'-(7-octynyl)-oxy)biphenyl (mono-8). This compound was prepared using a method similar to that described for **mono-6**. Quantity used: **7** (0.81 g, 2.7 mmol), **12** (0.7 g, 2.6 mmol), DCC (0.82 g, 3.9 mmol), and DMAP (0.48 g, 3.9 mmol) in CH_2Cl_2 (50 mL). Yield: 90%, 0.85 g (white crystal). IR (KBr, cm^{-1}): 3285 (m, $\nu_{\text{HC}\equiv}$), 2112 (w, $\nu_{\text{C}=\text{C}}$), 1737 (s, $\nu_{\text{C}=\text{O}}$), 1255 (s, ν_{COC}), 640 (w, $\gamma_{\text{HC}\equiv}$). ^1H NMR (500 MHz, CDCl_3 , δ from TMS, ppm): 0.90 (t, 3H, $J = 7.0$ Hz, CH_3), 1.25–1.91 (m, 18H, CH_2), 1.95 (t, 1H, $J = 2.6$ Hz, $\text{HC}\equiv$), 2.22 (dt, 2H, $J = 7.0$, $\text{HC}\equiv\text{CCH}_2$), 4.01 (t, 2H, $J = 6.5$ Hz, OCH_2), 4.10–4.22 (m, 2H, CH_2), 4.87 (dm, 1H, $J_{\text{HF}} = 49.1$ Hz, $\text{OCH}_2\text{C}^*\text{HF}$), 6.97 (d, 2H, $J = 8.7$ Hz, ph), 7.01 (d, 2H, $J = 8.9$ Hz, ph), 7.24 (d, 2H, $J = 8.6$ Hz, ph), 7.51 (d, 2H, $J = 8.7$ Hz, ph), 7.58 (d, 2H, $J = 8.7$ Hz, ph), 8.18 (d, 2H, $J = 8.8$ Hz, ph). ^{13}C NMR (125 MHz, CDCl_3 , δ from TMS, ppm): 14.02, 15.56, 16.41, 22.54, 24.52, 26.09, 29.07, 29.46, 29.50, 31.63, 31.64, 67.93, 69.65, 70.01, 94.77, 91.93 (d, $J_{\text{CF}} = 171.8$ Hz), 114.45, 114.87, 121.94, 122.39, 122.53, 127.74, 128.15, 132.37, 133.43, 138.64, 150.01, 159.01, 163.14. ^{19}F NMR (470 MHz, CDCl_3 , δ , ppm): -187.40.

4-[4-((S)-2-Fluorooctyloxy)benzyloxy]-4'-(12-dodecyloxy)biphenyl (mono-9). This compound was prepared using a method similar to that described for **mono-6**. Quantity used: **8** (0.65 g, 1.9 mmol), **12** (0.50 g, 1.9 mmol), DCC (0.77 g, 3.7 mmol), and DMAP (0.46 g, 3.7 mmol) in 5 mL of CH_2Cl_2 . The residue was purified by column chromatography (silica gel, benzene/hexane = 2) followed by recrystallization from ethanol. Yield: 0.87 g, 76% (white solid). IR (KBr, cm^{-1}): 3300 (m, $\nu_{\text{HC}\equiv}$), 2130 (w, $\nu_{\text{C}=\text{C}}$), 1730 (s, $\nu_{\text{C}=\text{O}}$), 1254 (s, ν_{COC}), 642 (w, $\gamma_{\text{HC}\equiv}$). ^1H NMR (500 MHz, CDCl_3 , δ from TMS, ppm): 0.90 (t, 3H, $J = 6.9$, CH_3), 1.25–1.91 (m, 26H), 1.94 (t, 1H, $J = 2.6$, $\text{HC}\equiv$), 2.17–2.22 (m, 2H), 4.00 (t, 2H, $J = 6.5$ Hz, OCH_2), 4.11–4.22 (m, 2H), 4.86 (dm, 1H, $J_{\text{HF}} = 50.5$ Hz, $\text{OCH}_2\text{C}^*\text{HF}$), 6.96 (d, 2H, $J = 8.7$ Hz, ph), 7.01 (d, 2H, $J = 8.9$ Hz, ph), 7.24 (d, 2H, $J = 8.7$ Hz, ph), 7.51 (d, 2H, $J = 8.7$ Hz, ph), 7.58 (d, 2H, $J = 8.5$ Hz, ph), 8.17 (d, 2H, $J = 8.9$ Hz, ph). ^{13}C NMR (125 MHz, CDCl_3 , δ from TMS, ppm): 14.05, 15.58, 16.42, 22.56, 24.56, 26.07, 24.51, 26.76, 29.07, 29.39, 29.44, 29.52, 30.91, 31.60, 31.67, 67.98, 69.66, 70.04, 94.75, 91.91 (d, $J_{\text{CF}} =$

Scheme 2



171.6 Hz), 114.44, 114.85, 121.97, 122.41, 122.50, 127.71, 128.12, 132.36, 133.40, 138.63, 149.99, 158.61, 162.95. ^{19}F NMR (470 MHz, CDCl_3 , δ , ppm): -187.47.

Polymerization. A typical procedure for the polymerization is as follows: under argon atmosphere, 4.8 mL of triethylamine (NEt_3) was added to 15 mg (0.03 mmol) of (bicyclo[2,2,1]hepta-2,5-diene)chlororhodium (I) dimer, $[\text{Rh}(\text{NBD})\text{Cl}]_2$, in a Schlenk flask with stirring. After aging the solution for 30 min at room temperature, 200 mg (0.33 mmol) of *mono-9* and 5 mL of THF were added. Polymerization was carried out for 24 h at 60 °C. The solution was poured into a large amount of methanol and stirred for 24 h. After filtration, the polymer was further washed with 25 mL of a mixed solution of THF/EtOH = 1/24 and dried under vacuum to afford brown powder.

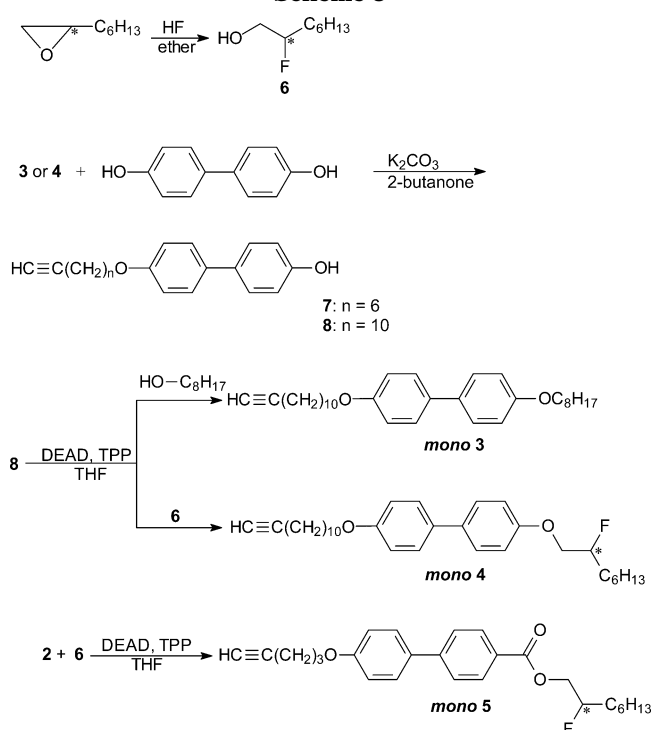
Results and Discussion

Synthesis of the Type 1 Monomers. The synthetic routes of the type 1 monomers having two aromatic rings in mesogenic core are shown in Schemes 2 and 3.

Compound **1** was prepared by etherification of 4-cyano-4'-hydroxybiphenyl in the presence of K_2CO_3 and KI in DMF. Then the cyano group in **1** was converted into a carboxylic group by KOH in mixed solution of ethanol/water to give **2**. 8-Bromo-1-octyne (**3**) or 12-bromo-1-dodecyne (**4**) was prepared by reacting dibromohexane or dibromodecane with sodium acetylide in DMF, respectively. Compounds **2** and **5** were coupled with (*S*)-octanol according to the Mitsunobu reaction using DEAD and TPP followed by silica gel column chromatography and recrystallization to afford *mono-1* ($n=3$) and *mono-2* ($n=10$). This reaction is characterized by S_N2 -type Walden inversion at the chiral center but with no racemization, resulting in the formation of ester with (*R*)-configuration.²⁵

4,4'-Biphenyldiol is etherified with **3** and **4** in the presence of K_2CO_3 and KI to afford **7** ($n=6$) and **8** ($n=$

Scheme 3



10). Compound **8** is then reacted with the fluorine-containing compound **6** or 1-octanol according to the Mitsunobu reaction to yield *mono-3* and *mono-4* as monomers.

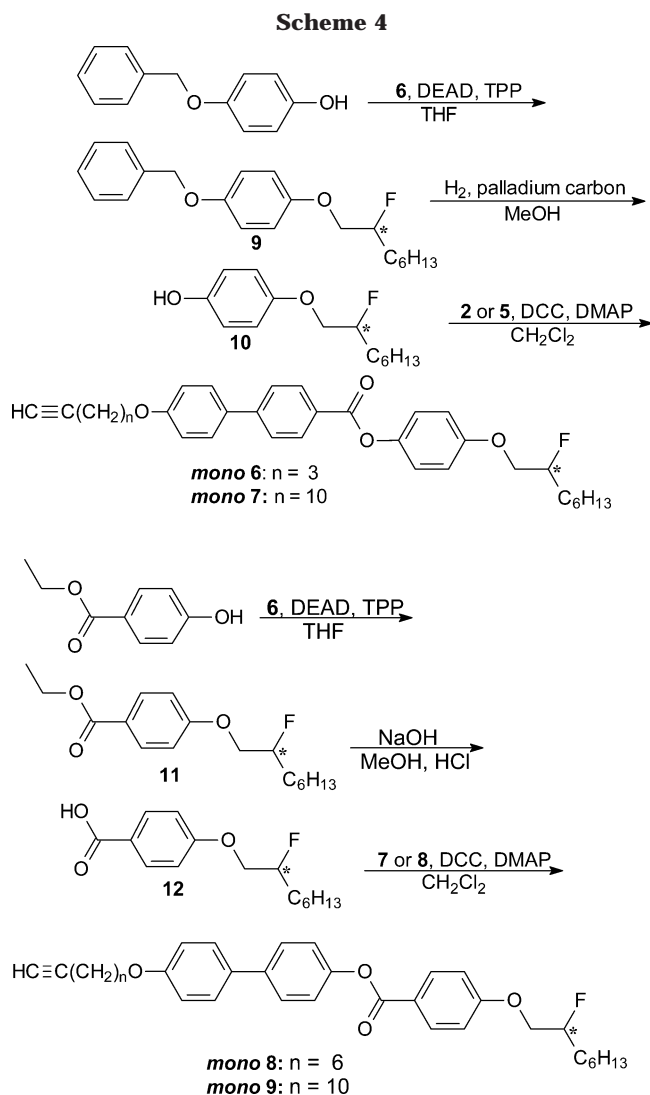
Compound **2** was esterified with a fluorine-atom-containing compound **6** by combination of DEAD and TPP to yield *mono-5* with (*S*)-configuration.

Synthesis of the Type 2 Monomers. Type 2 monomers having three aromatic rings in the mesogenic core are outlined in Scheme 4. *Mono-6* and *mono-7* structurally resemble *mono-8* and *mono-9*, but the esters of the joint group in the mesogen face different directions, so the LC director along the ester group faces in the opposite direction to those of *mono-8* and *mono-9*.

The first step of *mono-6* and *mono-7* syntheses consists of etherification of 4-benzyloxyphenol with **6** by DEAD and TPP to yield **9** with (*S*)-configuration. Compound **9** was then deprotected using H_2 and Pd/C in methanol to obtain **10** with a hydroxyl group. Then compound **10** was coupled with **2** or **5** using DCC and DMAP to synthesize *mono-6* ($n=3$) or *mono-7* ($n=10$), respectively.

p-Hydroxybenzoate was esterified with **6** by the Mitsunobu reaction to yield **11** with (*S*)-configuration. Ethyl moiety in **11** was removed by NaOH in mixed solution of methanol/water to give **12**. Compound **12** was then esterified with compound **7** or **8** by DCC and DMAP in CH_2Cl_2 to afford *mono-8* ($n=6$) or *mono-9* ($n=10$), respectively.

Polymerization. $\text{Fe}(\text{acac})_3\text{-AlEt}_3$, a Ziegler-Natta catalyst, and $\text{MoCl}_5\text{-Ph}_4\text{Sn}$, a metathesis catalyst, can polymerize monosubstituted acetylene derivatives. In particular, very high molecular weights can be obtained by the Fe catalyst in the polymerization of phenylacetylene or 4-phenyl-1-butyne.²⁷ However, these systems are not valid for polymerizations of monomers with ester groups due to the fact that metal ions react with the ester group in the monomer, which results in deactivation of the catalyst. Thus, we adopted a rhodium



complex catalyst, $[\text{Rh}(\text{NBD})\text{Cl}]_2$, where NBD stands for 2,5-norbornadiene, for polymerization of the acetylene monomers with FLC substituent because the Rh complex catalyst has no poisoning interaction with the polar ester group. Polymerizations of the acetylene monomers (**mono-1–9**) were carried out in triethylamine/THF at 60 °C for 24 h. After the polymerization reaction, lower molecular weight fractions were removed by washing with methanol followed by filtration to yield brown solid. All the polymers synthesized were fusible and soluble in common organic solvents such as THF and chloroform. The polymerization results are summarized in Table 2.

Number-average molecular weights (M_n) of the different polymers vary between 4500 and 21 600. The

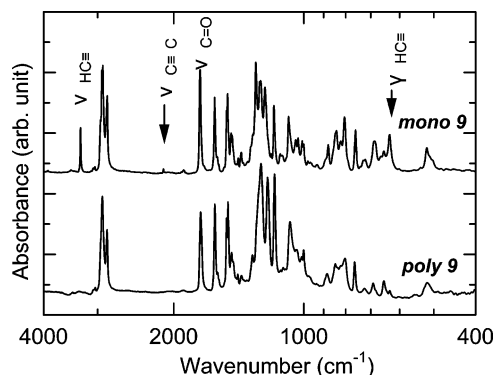


Figure 1. FT-IR spectra of **mono-9** and **poly-9**.

Table 3. Results of Optical Absorption and CD Spectroscopy Measurements

polymer	optical absorption ^a		CD ^a	
	λ (nm)	ϵ ($\times 10^4$)	λ (nm)	$\Delta\epsilon$
poly-1	292	2.32	284	-1.09
poly-2	295	1.66	330, 246	-2.40, -3.57
poly-3	296	2.01		
poly-4	273	3.76	292	-1.41
poly-5	294	2.84	299	0.75
poly-6	296	2.76	296, 270	-1.25, 3.90
poly-7	301	2.60	293, 260	-1.21, 0.54
poly-8	292	3.10	282	-2.1
poly-9	268	9.10	280	-5.1

^a Maximum values; measured in CHCl_3 .

molecular weight distributions (MWD, calculated by M_w/M_n , M_w = weight average molecular weights) are 1.5–3.7.

Living polymerization of phenyl acetylene using an Rh complex catalyst was reported by Masuda et al.²⁹ Percec and Oda performed living polymerization of vinyl monomers bearing FLC substituents with controlled degree of polymerization (DP).³⁰ In our study, we were not able to obtain polymer by living polymerization. This may be due to the fact that the steric repulsion between bulky substituents of the FLC during the polymerization in the solvent resulted in a decrease of polymerization activity.

In the IR spectra, the polymer shows no absorptions characteristic of the acetylene moiety in the monomer, $\text{HC}\equiv$ stretching at 3300 cm^{-1} , $\text{C}\equiv\text{C}$ symmetry stretching vibration at 2100 cm^{-1} , and $\text{HC}\equiv$ out-of-plane vibration about 630 cm^{-1} for the monomers. IR spectra of **mono-9** and **poly-9** are shown in Figure 1. All the acetylene absorptions disappear in the IR spectra of the polymers, indicating that the polymerizations were performed successfully by reaction of the opening of the triple bond.

Results of absorption and CD (circular dichroism) spectroscopy measurements are summarized in Table 3. All of the polymers show a Cotton effect in CD spectra except **poly-3** (**poly-3** having no chiral moiety). Those results can be attributed to the presence of the optically active moiety in the LC substituents, and the asymmetry in the chiral center of the compounds is maintained after the polymerization. Only **poly-5** shows a positive Cotton effect in the CD; however, the reason for this is unclear.

In the ^1H NMR (500 MHz) spectra, no signals characteristic of the acetylenic moiety in the monomer, e.g., the triplet signal at 1.93 ppm originating from acetylene hydrogen ($\text{HC}\equiv$) as well as the $\text{C}\equiv\text{C}$ at 68 and 84 ppm

Table 4. NMR Results for Polymers

polymer	¹ H NMR ^a			¹³ C NMR ^a	¹⁹ F NMR ^b
	–C*HF– (<i>J</i> _{HF} in Hz) ^c	–C*HCH ₃ –	olefin ^{c,d}	–C*HF– (<i>J</i> _{CF} in Hz) ^c	–C*HF–
<i>poly-1</i>		5.10 (sextet)	6.07 (s, 0.96H ^e)		
<i>poly-2</i>		5.15 (sextet)	<i>f</i>		
<i>poly-3</i>			<i>f</i>		
<i>poly-4</i>	4.83 (d, 51.6)		<i>f</i>	91.52 (d, 172.1)	–187.74
<i>poly-5</i>	4.76 (d, 49.4)		6.05 (s, 0.79 H ^e)	91.55 (d, 172.5)	–187.76
<i>poly-6</i>	4.76 (d, 52.1)		6.14 (s, 0.10 H ^e)	91.53 (d, 172.2)	–187.47
<i>poly-7</i>	4.82 (d, 49.0)		6.10 (s, 0.10 H ^e)	91.92 (d, 171.9)	–187.46
<i>poly-8</i>	4.85 (d, 47.1)		<i>f</i>	91.48 (d, 171.8)	–187.36
<i>poly-9</i>	4.70 (d, 49.3)		<i>f</i>	91.56 (d, 172.6)	–187.45

^a Chemical shift value (δ , in CDCl₃, ppm from TMS), asterisk (*) = chiral center. ^b Trifluorotoluene was used as an internal standard (δ in CDCl₃). ^c d = doublet, s = singlet. ^d Olefin proton of cis form. ^e Integral value of proton signal in ¹H NMR. ^f Did not clearly appear.

in ¹³C NMR (125 Hz) appeared. These results indicate that an opening of the acetylenic carbon in the monomer catalyzed by the Rh complex catalyst gives a linear polymer with conjugated double bond. From the results of ¹H NMR spectra, **poly-1** and **poly-5–7** have peaks at 6.05–6.14 ppm characteristic of a proton attached to a cis double bond.²⁸ On the other hand, **poly-2–4**, **poly-8**, and **poly-9** show no peak corresponding to the cis form. This result suggests that **poly-1** and **poly-5–7** are predominantly cis configuration, and **poly-2–4**, **poly-8**, and **poly-9** were isomerized from the cis into trans configuration during the polymerization. In general, polymerization of acetylene monomer by Rh complex catalyst yields *cis*-rich polymer. The *cis*–*trans* isomerization during the acetylene polymerization is dependent on temperature. In this experiment, we attempted polymerizations of the monomers with relatively bulky substituents at reflux temperature so as to increase reactivity. The polymer main chains of **poly-1** and **poly-5–7** may be partly isomerized (cis content <100%) and showed an olefin proton signal around 6 ppm in the ¹H NMR due to residual cis content, while other polymer main chains were isomerized to trans configuration \approx 100% during the reaction. It is probable that polymerization at low temperature produces *cis*-rich polymers; however, in this case, higher molecular weight FLC polymers cannot be obtained.

In ¹H NMR measurement, a signal due to the hydrogen atom attached onto the chiral carbon appeared at 5.1 ppm as a sextet for **mono-1** and **mono-2**. The corresponding polymers, **poly-1** and **poly-2**, showed the same δ value signal at 5.1 ppm. Also, a doublet signal due to a hydrogen atom attached to the chiral carbon with a fluorine atom for **mono-4–9** appeared around 4.9 ppm, the signal was unchanged after polymerization. A signal due to the fluorine atom appeared around –187 ppm in ¹⁹F NMR (470 MHz) of all the monomers and polymers. A doublet signal appeared in the ¹³C NMR of **mono-4–9** and **poly-4–9** at 91.5 ppm due to C–F coupling (*J*_{CF} = 172 Hz). ¹H–¹⁹F heteronuclear Overhauser effect spectroscopy (HOESY) results indicate that the doublet at 4.9 ppm in the ¹H NMR (500 MHz) due to the proton on the chiral carbon and the signal at –187 ppm in ¹⁹F NMR (470 MHz) due to the fluorine atom attached onto the chiral center are correlated. NMR results of the polymers are summarized in Table 4.

The acetylene monomers **mono-1–5** showed no mesophase. The precursor **12** exhibited enantiotropic chiral nematic (N*) with fingerprint texture and unidentified smectic X (SmX) phases. This is probably due to the formation of a hydrogen-bonding dimer of **12**. **Mono-7** showed the focal conic fan-shaped texture of chiral

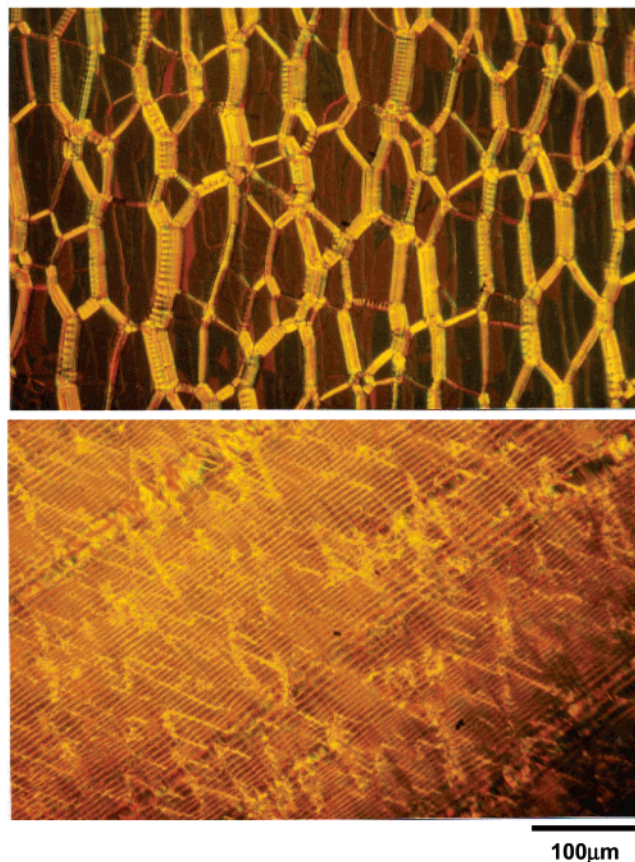


Figure 2. Polarizing optical micrographs of **mono-9**. Oily streak texture of chiral nematic (N*) phase at 159 °C (top). Line texture of chiral smectic C (SmC*) phase at 134 °C (bottom).

smectic A (SmA*) in the heating process, and it showed SmA* and the striated fan-shaped texture of chiral smectic B (SmB*) in the cooling process. In the SmA* phase, **mono-6** and **mono-7** showed a broad halo in the wide-angle region in XRD which can be ascribed to the distance between the molecules in the LC phase. The wide-angle halo became sharp in the SmB* phase due to the fact that the distances between the LC molecules were constant. This result supports the fact that **mono-6** and **mono-7** show no SmC* but show SmB* in the cooling process. **Mono-8** showed the fingerprint texture of the N* and the striated fan-shaped texture of the SmC* phases. On cooling from the isotropic phase, **mono-9** showed the N* and SmC* phases and two unidentified higher order smectic phases. The SmC* phase is observed in a wide temperature range for **mono-8** and **mono-9**. Figure 2 shows the typical N* and the SmC* textures of **mono-9**. Temperature-dependent

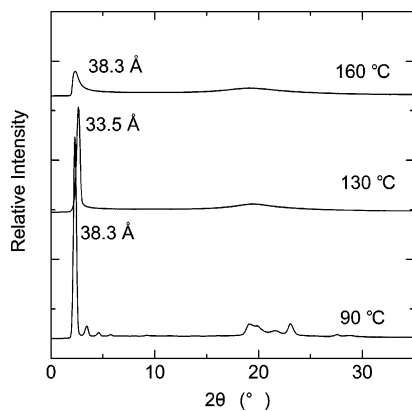


Figure 3. XRD patterns of *mono-9*.

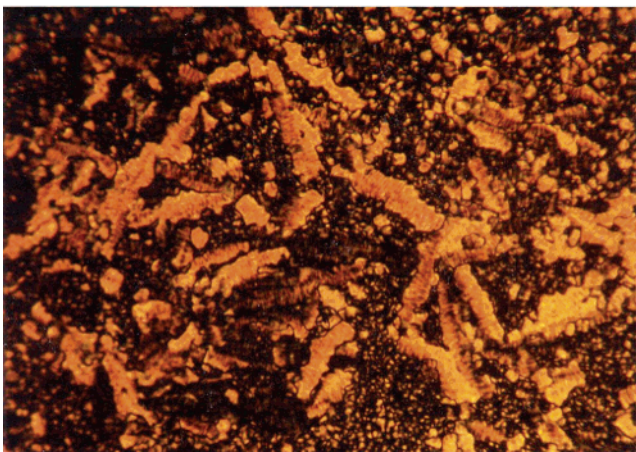
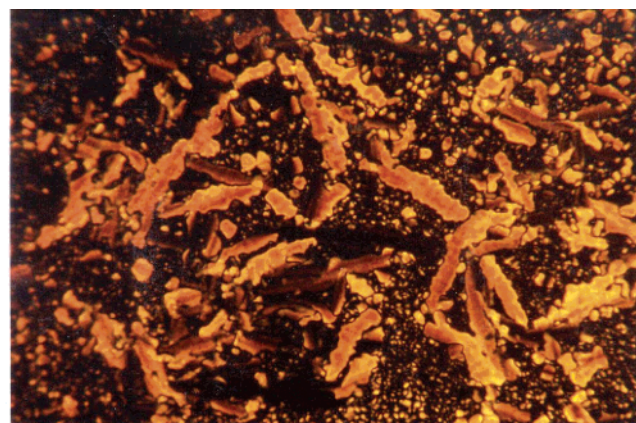


Figure 4. Polarizing optical micrographs of *poly-4*. Bñtonnets texture of SmA* at 140 °C (top). Striated bñtonnets texture of SmX at 120 °C (bottom).

XRD patterns were obtained from the powder sample of *mono-9* at 160, 130, and 90 °C (Figure 3).

Poly-1 (spacer length: $n = 3$) showed no liquid crystallinity. *Poly-2* (spacer length: $n = 10$) showed the sanded texture. *Poly-3* showed the SmA and SmX and *poly-4* showed the bñtonnets texture of the SmA* and the SmX phases during the cooling process, as shown in Figure 4. *Mono-6* showed no SmC*; on the other hand, *poly-6* of the corresponding polymer exhibited the SmC*. This is probably due to the LC side chains aligning themselves with the polyacetylene main chain, and this order allows the side chains to form an SmC* array. This phenomenon could be referred to the so-called polymer effects. XRD patterns of *poly-9* were

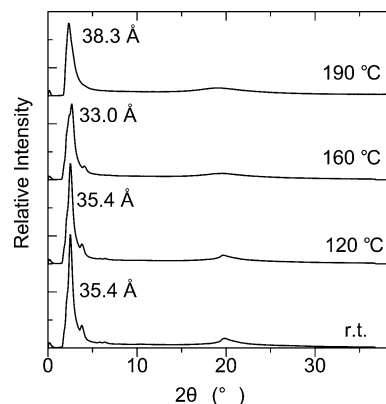


Figure 5. XRD patterns of *poly-9*.

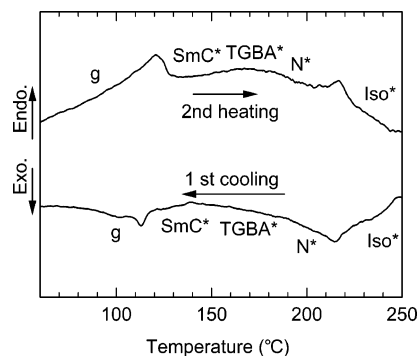


Figure 6. DSC curves of *poly-8*.

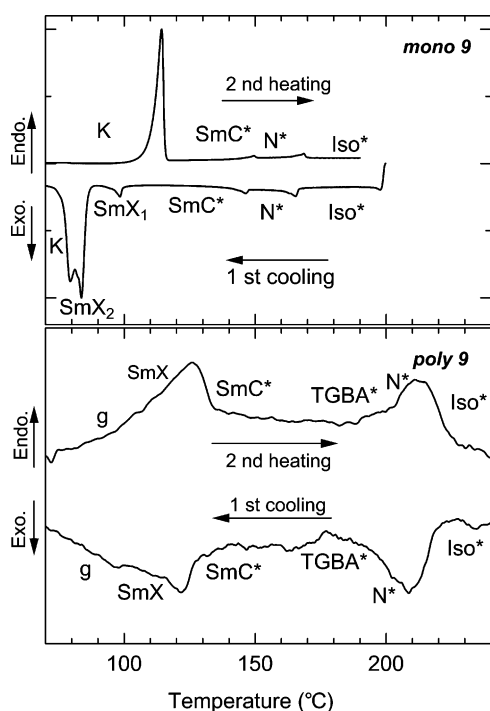
shown in Figure 5. When *poly-9* was allowed to cool from the isotropic state, the polymer showed the fingerprint texture typical of the N* phase and a filament texture at 193 °C under POM observation, as shown in Figure 8 (top). At the same time, the XRD pattern of *poly-9* measured in the LC phase at 190 °C gave two reflection peaks. The sharp peak at the small-angle region and broad halo at the wide-angle region correspond to a distance of 38.3 (layer spacing) and 4.62 Å (distance between side chains). This is a typical pattern of the smectic phase. In other words, a SmA-type layer structure exists in this phase for *poly-9*. The optical texture and the results of XRD measurement is due to *poly-9* forming twist grain boundary smectic A (TGBA*) phase, since the TGBA* phase possesses both characteristics of the N* and smectic A phases. The TGBA* helical axis is parallel to the smectic layer planes, and the director in the layer rotates discontinuously around the twist axis.²⁶ When temperature was allowed to cool to 160 °C, the d -spacing of the small-angle reflection decreased from 38.3 to 33.0 Å. This result suggests the formation of a tilted smectic phase. A parabolic texture of the SmC* phase for *poly-9* was observed in this temperature range under POM, as shown in Figure 8 (bottom). When the temperature was further cooled to 120 °C, the d -spacing of the small-angle reflection increased from 33.0 to 35.4 Å and the wide-angle reflection became sharp. This structure was unchanged in the glassy state.

Similarly, *poly-8* shows TGBA* in both cooling and heating processes. *Poly-8* also showed filament texture of the TGBA* and striated fan-shaped texture of the SmC* phases with enantiotropic nature; however, *poly-8* and *poly-9* showed no square grid pattern of the TGBC* phase. This is the first time the TGBA* phase has been observed in LC conjugated polymers. DSC thermograms of *poly-8* and *mono-9*, *poly-9* are shown in Figures 6

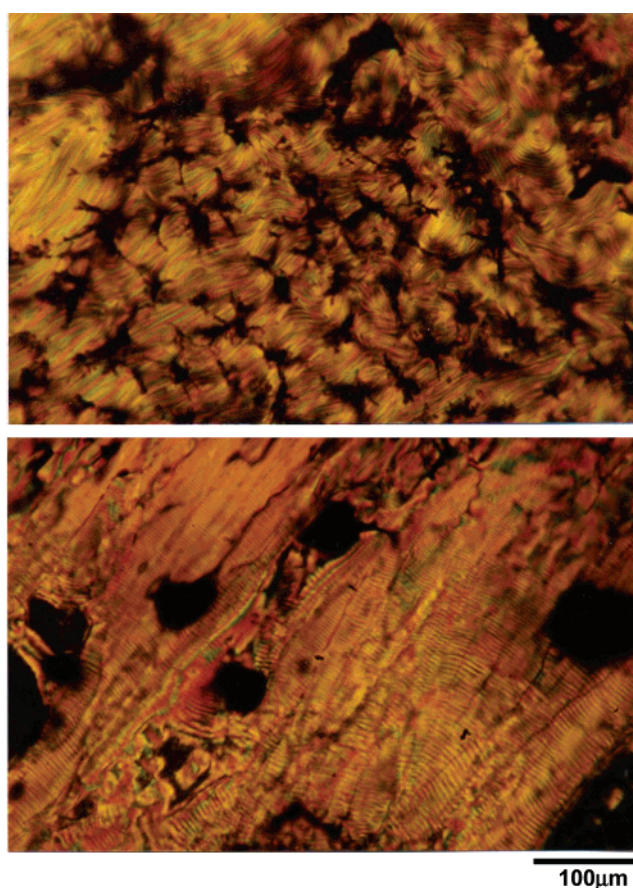
Table 5. Thermal Transition of Monomers and Polymers

compd	phase-transition temperature (°C)	
	heating	cooling
12	K·105·SmX 121·N*·138·Iso*	K·96·SmX·118·N*·135·Iso*
mono-6	K·102·SmB*·110·SmA*·181·Iso*	K·58·SmB*·101·SmA*·162·Iso*
mono-7	K·105·SmA*·165·Iso*	K·47·SmB*·93·SmA*·162·Iso*
mono-8	K·107·SmC*·130·N*·167·Iso*	K·87·SmC*·127·N*·164·Iso*
mono-9	K·114·SmC*·149·N*·168·Iso*	K·79·SmX ₂ ·84·SmX ₁ ·98·SmC* 147·N*·166·Iso*
poly-1	a	a
poly-2	g·52·SmX·87·Iso*	g· ^b SmX·61·Iso*
poly-3	g·144·SmA·164·Iso	g·142·SmX· ^b SmA·158·Iso
poly-4	g·121·SmA*·149·Iso*	g·117·SmX· ^b SmA*·144·Iso*
poly-5	g·80·SmA*·180·Iso*	g·78·SmC*·124·SmA*·140·Iso*
poly-6	g·135·SmA*·306·Iso*	g·111·SmC*·160·SmA*·305·Iso*
poly-7	g·120·SmA*·209·Iso*	g·110·SmX·118·SmC*·162·SmA* 203·Iso*
poly-8	g·121·SmC*· ^b TGBA*· ^b N*·217·Iso*	g·113·SmC*· ^b TGBA*· ^b N*·214·Iso*
poly-9	g·104·SmX·126·SmC*· ^b TGBA*· ^b N*·213·Iso*	g·97·SmX·121·SmC*· ^b TGBA*· ^b N*·208·Iso*

^a No LC phase. ^b No distinct transition was observed in DSC. K, crystal; SmX, unidentified LC phase; SmA, smectic A phase; SmA*, chiral smectic A phase; SmB*, chiral smectic B phase; SmC*, chiral smectic C phase; TGBA*, twist grain boundary smectic A* phase; N*, chiral nematic phase; Iso*, isotropic.

Figure 7. DSC curves of *mono-9* and *poly-9*.

and 7, respectively. Thermal transitions of *mono-8* are enantiotropic, and three peaks associated, respectively, with the Iso*–N*, N*–SmC*, and SmC*–K (K: crystal) transitions during the heating and cooling scans appear. An exothermic peak due to cis–trans isomerization of the polyacetylene main chain was observed around 180 °C during the first heating process of the DSC measurements for *poly-1*, *poly-5*, *poly-6*, and *poly-7*. In the second heating scan of DSC thermograms, *poly-8* displays two peaks in both the heating and cooling cycle. In the heating process, two peaks at 121 and 217 °C were observed, which can be ascribed to the g–SmC* (g = glassy state) and N*–Iso* transitions; however, no clear peak of the SmC*–TGBA* transition was observed. The phase transition is second order in nature; on the other hand, *poly-8* shows visible change of the optical texture at 168 °C under the POM observations. Also, a peak corresponding to the phase transition from TGBA* to N* did not appear clearly in the DSC measurements. This can be due to the fact that TGBA* is a frustrated LC phase. *Mono-9* shows three peaks

Figure 8. Polarizing optical micrographs of *poly-9*. Filament texture of twist grain boundary (TGBA*) phase at 193 °C (top). Parabolic texture of SmC* phase at 165 °C (bottom).

due to K–SmC*, SmC*–N*, and N*–Iso* in the heating process and five peaks due to Iso*–N*, N*–SmC*, SmC*–SmX₁, SmX₁–SmX₂, and SmX₂–K during the cooling process. *Poly-9* showed two distinct peaks due to the SmX–SmC* and N*–Iso* transitions at 126 and 213 °C on the second heating, respectively, but SmC*–TGBA* and TGBA*–N* transitions did not clearly appear in the DSC measurements. *Poly-6* and *poly-7*, with the ester group facing the opposite direction from those of *poly-8* and *poly-9*, show no TGBA* phase, and they exhibit monotropic SmC* phase. Phase-transition temperatures of 12, the monomers, and the polymers are summarized in Table 5.

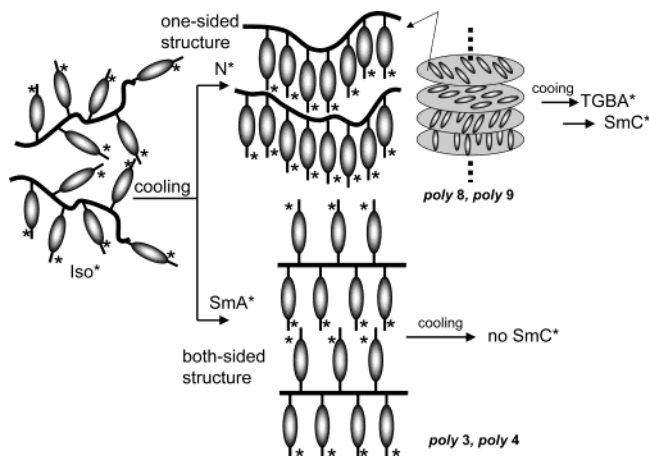
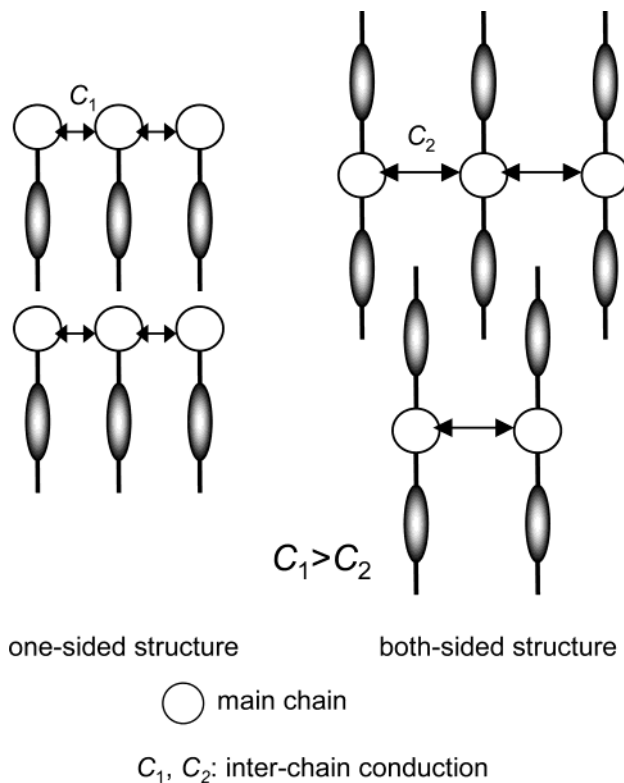


Figure 9. Possible change of the LC structures.

Generally there are two possible structures for the LC-substituted polyacetylene derivatives, where the side chains are located on either one side or both sides of the main chain in the LC layers. They are abbreviated as “one-sided” and “both-sided” structures, respectively. In the case of **poly-3**, molecular mechanics (MM) calculations imply that the d -space (interlayer distance) of the one-sided and both-sided structures is 34.7 and 67.5 Å, respectively. XRD measurements gave a d -space of 55.2 Å, which is close to that predicted for the both-sided structure. **Mono-9** shows peaks at 38.3 (160 °C, N*), 33.5 (130 °C, SmC*), and 38.3 Å (90 °C, SmX₁), and **poly-9** shows peaks at 38.3 (190 °C, N*), 33.0 (160 °C, SmC*), and 35.4 Å (120 °C: SmX, and room temperature: glassy state) in XRD measurements. These results suggest that **poly-9** forms the one-sided structure because the layer spacing of **mono-9** and **poly-9** show similar values in XRD measurement in each LC temperature range. Taking into account the results of the XRD measurements of the monomers and the polymers and the MM calculations, it can be argued that **poly-3** and **poly-4** have the both-sided structure while **poly-8** and **poly-9** the one-sided structure.

In the cooling process, **poly-8** and **poly-9** show first the N* phase after the Iso*. The nematic phase has low order and high symmetry compared to the other liquid crystal phases³¹ as well as the lowest viscosity. The N* phase is the chiral form of the nematic phase. The phase consists of local nematic layers which are continuously twisted with respect to each other and show an overall helical structure. The long molecular axis of the asymmetric structure is oriented to a single direction in each layer. The property strongly depends on the chirality of the mesogen. In the case of the LC polymers, the asymmetric side chains align to one direction along the director of each layer in the N* phase, and it is possible to form one-sided structure for **poly-8** and **poly-9** in the N*. The polymers can transform into the TGBA*, SmC*, and glassy state maintaining the one-sided structure of the N*. On the other hand, **poly-3** and **poly-4** show no N* phase in the cooling process. They first form the SmA* with bilayer structure after Iso* in the cooling process and can be transformed into the glassy state via the SmX with both-sided structure. Possible LC structures along with the phase transitions are shown in Figure 9.

We performed iodine doping of the polymers in the glassy state (solid state), which retains the former liquid crystalline order. The polymer samples for the conduc-



one-sided structure

both-sided structure

○ main chain

C_1, C_2 : inter-chain conduction

Figure 10. Schematic illustration of possible conduction of one-sided and both-sided polymer structures.

tivity measurement were prepared by gradually cooling to room temperature from the isotropic phase. Although the color of the sample changed to dark purple after the doping, the optical texture was unchanged.

Electrical conductivities of **poly-3**, **poly-4**, **poly-8**, and **poly-9** after iodine doping were 3.5×10^{-7} , 7.3×10^{-7} , 5.3×10^{-5} , and 1.8×10^{-4} S/cm, respectively. This result indicated that the polymers of the one-sided structure showed 100–500 times higher conductivities than the polymers of the both-sided structure. The distance between the main chains of the polymers with the one-sided structure is shorter than that of the polymers with the both-sided structure. This can cause better electrical conduction between the polymer main chains by the hopping mechanism than the polymer with both-sided structure. This would cause **poly-8** and **poly-9** with the one-sided structure to give higher electrical conductivities than **poly-3** and **poly-4** with the both-sided structure. A possible conduction of the one-sided structure and the both-sided structure of the polymers is shown in Figure 10.

In conclusion, novel LC polyacetylene derivatives have been synthesized by introducing achiral LC groups or chiral LC groups into the side chains. Three polymers (**poly-5–7**) showed a monotropic SmC* phase, and two polymers (**poly-8**, **poly-9**) showed an enantiotropic SmC* phase, whose temperature range was quite wide (in the range of 50 °C). This is the first report of polyacetylene derivatives showing SmC*. Polymers with SmC* have the ability to respond more quickly to an external electric field than non-FLC ones. Therefore, the conjugated polymers bearing FLC substituents can be used in electrooptical applications such as unique electronic devices with high-speed response. Also, it may be possible to use them in an FLC memory type display.

Acknowledgment. We thank Professor Hideki Shirakawa for valuable discussions and advice. We also thank Messrs. Yutaka Bannai and Jyunya Murakami (Institute of Materials Science, U. Tsukuba) for their assistance. This work was supported by Grant-in-Aids for Scientific Research from the Ministry of Education, Culture, Sports, Science and Technology, Japan, and "Promotion of Creative Interdisciplinary of Materials Science for Novel Functions" of the 21st century Center of Excellence (COE) program of the Ministry of Education, Culture, Sports, Science and Technology, Japan, and The Ogasawara Foundation for Promotion of Science and Engineering.

References and Notes

- (1) Akagi, K.; Shirakawa, H. *Macromol. Symp.* **1996**, *104*, 137.
- (2) Akagi, K.; Shirakawa, H. *The Polymeric Materials Encyclopedia. Synthesis, Properties and Applications*; CRC Press: Boca Raton, FL, 1996; Vol. 5, p 3669.
- (3) Akagi, K.; Shirakawa, H. In *Electrical and Optical Polymer Systems: Fundamentals, Methods, and Applications*; Wise, D. L., et al., Eds.; Marcel Dekker: New York, 1998; Vol. 28, p 983.
- (4) Kuroda, H.; Goto, H.; Akagi, K.; Kawaguchi, A. *Macromolecules* **2002**, *35*, 1307.
- (5) Huang, Y. M.; Yip Lam, J. W.; Leung Cheuk, K. K.; Ge, W.; Tang, B. Z. *Mater. Sci. Eng. B: Solid-State Mater. Adv. Technol.* **2001**, *B85*, 122.
- (6) Akagi, K.; Goto, H.; Murakami, J.; Silong, S.; Shirakawa, H. *J. Photopolym. Sci. Technol.* **1999**, *12*, 269.
- (7) Akagi, K.; Goto, H.; Hayashi, A. *Synth. Met.* **1999**, *103*, 2291.
- (8) Tang, B.-Z.; Kong, X.-X.; Feng, X.-D. *Chin. J. Polym. Sci.* **1999**, *17*, 289.
- (9) Koltzenburg, S.; Stelzer, F.; Nuyken, O. *Macromol. Chem. Phys.* **1999**, *200*, 821.
- (10) Lam, W.-Y.; Kong, X.; Tang, B.-Z. *Polym. Mater. Sci. Eng.* **1999**, *80*, 159.
- (11) Akagi, K.; Shirakawa, H. *Curr. Trends Polym. Sci.* **1997**, *2*, 107.
- (12) Iino, K.; Goto, H.; Akagi, K.; Shirakawa, H.; Kawaguchi, A. *Synth. Met.* **1997**, *84*, 967.
- (13) Goto, H.; Akagi, K.; Shirakawa, H. *Synth. Met.* **1997**, *84*, 373.
- (14) Oh, S.-Y.; Akagi, K.; Shirakawa, H. *Hwahak Konghak* **1996**, *34*, 154.
- (15) Oh, S.-Y.; Akagi, K.; Shirakawa, H. *Hwahak Konghak* **1996**, *34*, 70.
- (16) Shirakawa, H.; Kadokura, Y.; Goto, H.; Oh, S.-Y.; Akagi, K. *Mol. Cryst. Liq. Cryst.* **1994**, *255*, 213.
- (17) Le Moigne, J.; Hilberer, A.; Kajzar, F.; Thierry, A. *NATO ASI Ser., Ser. E: Appl. Sci.* **1991**, *194*, 327.
- (18) Oh, S.-Y.; Akagi, K.; Shirakawa, H.; Araya, K. *Macromolecules* **1993**, *26*, 6203.
- (19) Akagi, K.; Goto, H.; Kadokura, Y.; Shirakawa, H.; Oh, S.-Y.; Araya, K. *Synth. Met.* **1995**, *69*, 13.
- (20) Akagi, K.; Goto, H.; Shirakawa, H.; Nishizawa, T.; Masuda, K. *Synth. Met.* **1995**, *69*, 33.
- (21) Akagi, K.; Goto, H.; Shirakawa, H. *Polym. Prepr. (Am. Chem. Soc., Div. Polym. Chem.)* **1996**, *37*, 62.
- (22) Dai, X.-M.; Goto, H.; Akagi, K. *Mol. Cryst. Liq. Cryst.* **2001**, *365*, 347.
- (23) Akagi, K.; Goto, H.; Shirakawa, H. *Synth. Met.* **1997**, *84*, 313.
- (24) Nohira, H.; Nagamura S.; Kamei, M. *Mol. Cryst. Liq. Cryst.* **1990**, *180B*, 379.
- (25) Mitsunobu, O.; Yamada, M. *Bull. Chem. Soc. Jpn.* **1967**, *40*, 2380.
- (26) Goodby, J. W.; Waugh, M. A.; Stein, S. M.; Chin, E.; Pindak, R.; Patel, J. R. *J. Am. Chem. Soc.* **1989**, *111*, 819.
- (27) Oh, S.-Y.; Oguri, F.; Akagi, K.; Shirakawa, H. *J. Polym. Sci., Part A: Polym. Chem. Ed.* **1993**, *31*, 781.
- (28) Simionescu, C. I.; Percec, V.; Dumitrescu, S.; *J. Polym. Sci., Part A: Polym. Chem. Ed.* **1977**, *15*, 2497.
- (29) Miyake, M.; Mitsui, Y.; Masuda, T. *Macromolecules* **2000**, *33*, 6636.
- (30) Percec, V.; Oda, H. *Macromolecules* **1994**, *27*, 12.
- (31) Dierking, I. *Texture of Liquid Crystals*; WILEY-VCH: Weinheim, 2003; p 7.

MA035765G